Reprinted from Journal of the Optical Society of America B, Vol. 1, p. 723, October 1984

Angular radiation pattern of Smith–Purcell radiation

A. Gover, P. Dvorkis, and U. Elisha

Department of Electron Devices and Electromagnetic Radiation, Faculty of Engineering, Tel Aviv University, Ramat-Aviv 69978, Tel Aviv, Israel

Received February 16, 1984; accepted June 15, 1984

The power radiation pattern of Smith–Purcell radiation is measured at various latitudes and azimuth angles relative to the electron beam. The experimental data are used to evaluate the various models and the physical mechanisms previously suggested to describe Smith–Purcell radiation. Good agreement is observed between the experimental data and the theoretical curves derived from Van den Berg's analysis [J. Opt. Soc. Am. 63, 1588 (1973)]. The radiation mechanism proposed by Salisbury [J. Opt. Soc. Am. 60, 1279 (1970)] was analyzed and shown to be too small to account for the measured radiation. The experiment and Van den Berg's theory predict stronger emission at azimuthal angles off the plane perpendicular to the gratings. This observation leads to conclusions regarding the design of optical cavities for Smith–Purcell free-electron lasers and orotron millimeter-wavelength-radiation tube devices.

INTRODUCTION

We report the experimental and the theoretical interpretation of Smith–Purcell radiation experiments, which were carried out in our laboratory using a 60- to 100-KeV low-current electron beam and a variety of optical gratings. We put special emphasis on quantitative measurement of the radiation intensity and the radiation pattern. These data were used in order to evaluate the validity of various models and physical mechanisms that have been suggested to describe the Smith–Purcell effect. Because of the intimate relation between spontaneous and stimulated emission from free electrons,[1,2] the spontaneous-emission radiation data can be used to estimate the feasibility[2] of devices based on stimulated emission of Smith–Purcell radiation [Smith–Purcell free-electron lasers (FEL's)].[3–5] Here, we use these data to draw conclusions on the optimal design of resonator structures for such devices and for the closely related millimeter-wave tube device, the orotron.[6–9]

The basic configuration of the Smith–Purcell radiation effect is described in Fig. 1. An electron beam propagates parallel and close to the surface of an optical grating and perpendicular to the grating rulings. At any angle η relative to the plane perpendicular to the beam direction (*viz.*, $90° - \eta$ angle relative to the beam direction), radiation is emitted at a wavelength

$$\lambda_n = -\frac{D}{n}(c/v_0 - \sin \eta), \tag{1}$$

where D is the grating period, v_0 is the electron velocity, and n is a negative integer.

Various models and mechanisms have been proposed to explain the experimentally observed effect. Smith and Purcell explained the dispersion relation [Eq. (1)] in terms of a Huygens wave construction of the radiation emitted by the oscillating positive-image charge of the electron inside the conductive grating.[10] Ishiguro and Tako[11] used the oscillating-dipole model to calculate the radiation power and the radiation pattern using the known radiation formula of a moving dipole. Their calculations did not fit well with the measured Smith–Purcell radiation power and radiation pattern.

Since the image-charge model requires that the electrons move close to the grating (less than the grating period), only a small fraction of a finite-cross-section electron beam shot parallel to the grating will contribute significantly to the radiation. This motivated Salisbury[12] to offer an alternative mechanism to explain the Smith–Purcell radiation effect. According to Salisbury, some of the electrons in the electron beam hit the grating surface at a shallow angle and are reflected by the tops of the rulings, forming current sheets with a periodicity that is determined by the grating period. The space-charge electric field that is associated with the reflected sheet-current beamlets applies a periodic force on the other electrons across the incoming beam and forces them to oscillate. Salisbury reported experimental results that he claimed supported his model. However, no other independent study has confirmed his result to our knowledge. Furthermore, a complete quantitative calculation of the strength of Salisbury's mechanism was not given.

A useful model for solving the Smith–Purcell radiation problem was introduced by Toraldo di Francia,[13] who analyzed the radiation effect as a regular-grating diffraction problem in which the incoming wave is an evanescent wave that appears when the moving electron point charge is expanded into its Fourier components. This presentation of the Smith–Purcell radiation problem was further improved by Van den Berg,[14] who rigorously solved the Maxwell equations with the boundary conditions of an optical grating (assuming an ideal-conductor sinusoidal surface). Matching boundary conditions at the electron-beam coordinates resulted in an integral equation that was solved numerically and presented graphically in Ref. 14 for some exemplary parameters. Van den Berg's analysis seems to be the most rigorous quantitative description of Smith–Purcell radiation. However, its quantitative predictions were not compared with experiments.

A number of experimental studies of the Smith–Purcell radiation effect have been carried out since Smith and Purcell's experiment.[15,16] All these studies confirmed the basic

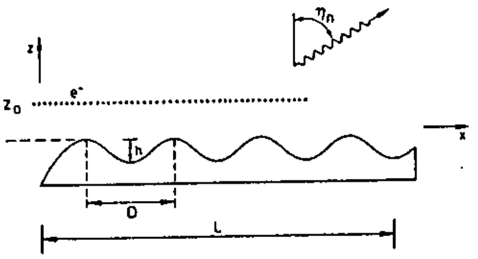

Fig. 1. Schematic of the Smith-Purcell radiation effect.

radiation condition [Eq. (1)]. However, little attempt was made to compare the quantitative power measurements with the predictions of the different theoretical models.

In this paper we base our experimental interpretation on Van den Berg's model. The main features of the measured Smith–Purcell radiation pattern at various latitude and azimuth angles fit well with the theoretical curves derived from interpolation of Van den Berg's example data.

In order to check Salisbury's model, we derive explicit expressions based on the known spontaneous-emission formulas of FEL's to account for the radiation emission resulting from the space-charge-force radiation mechanism. It was found that the predicted power emission resulting from this mechanism is orders of magnitude lower than the power measured experimentally. We conclude that Salisbury's model is irrelevant for the parameters of our experiment and probably for all previous Smith–Purcell experiments.

The experimental results in agreement with Van den Berg's model indicate stronger emission at azimuthal angles ζ off the plane that includes the electron-beam line and that is perpendicular to the grating. We point out the relevance of this observation to the resonator design for Smith–Purcell FEL's and orotrons.

THEORETICAL MODEL

Our theoretical model is based on the theory of Van den Berg.[14] The electromagnetic radiation on top of the gratings (Fig. 1) is given in terms of a Floquet mode series:

$$\mathbf{E}(\gamma, t) = (2\pi^2)^{-1}\,\mathrm{Re}\int_0^\infty \mathrm{d}\omega \int_{-\infty}^{\infty} \mathrm{d}k_y \mathcal{E}(x, y, k_y, \omega) \times \exp(ik_y y - i\omega t), \tag{2}$$

$$\mathcal{E}(x, y, k_y, \omega) = \sum_{n=-\infty}^{\infty} \mathcal{E}_n(k_y, \omega)\exp(ik_{xn}x + ik_{zn}z), \tag{3}$$

where

$$k_{xn} = k_{x0} + n2\pi/D, \tag{4a}$$

$$k_{zn} = (k^2 - k_y{}^2 - k_{xn}{}^2)^{1/2}, \tag{4b}$$

where $k = \omega/c$.

The zero-order space harmonic ($n = 0$) is chosen to be synchronous with the ω frequency Fourier component of the single-electron current $-ev_0\delta(x - v_0t, y, z - z_0)\hat{i}_x$:

$$\mathbf{J}(x, z, \omega) = -e\exp\left(i\frac{\omega}{v_0}z\right)\delta(z - z_0)\hat{i}_x \tag{5}$$

so that $k_{x0} = \omega/v_0$. It follows from Eqs. (4) that this space harmonic is necessarily nonradiating (evanescent in the z direction) since $k^2 - k_y{}^2 - (\omega/v_0)^2 < 0$. However, some of the negative-order space harmonics (diffraction orders) may be radiative if $k^2 - k_y{}^2 - k_{xn}{}^2 > 0$. The radiation directions can be defined in terms of the angular coordinate systems (η_n, ζ_n), which are illustrated in Fig. 2:

$$k_{xn} = k\sin\eta_n, \tag{6a}$$

$$k_{yn} = k\cos\eta_n\sin\zeta_n, \tag{6b}$$

$$k_{zn} = k\cos\eta_n\cos\zeta_n. \tag{6c}$$

The synchronization condition $\omega/v_0 = k_{x0}$ together with Eqs. 4(a) and 6(a) are sufficient to determine the radiation condition [Eq. (1)]. Clearly, only negative diffraction orders ($n < 0$) can radiate. Radiation is possible at all wavelengths λ and orders n that satisfy the inequality $|\sin\eta_n| = |(c/v_0) + (n\lambda/D)| < 1$. The radiation wavelength λ is only a function of the angle η and is independent of ζ. Consequently, Smith–Purcell radiation appears as a rainbow of continuously varying colors (wavelengths); each color is emitted along directions that define a half-cone of half-angle $\pi/2 - \eta$ whose axis lies along the beam-propagation direction.

Although the radiation (dipersion) condition [Eq. (1)] is derived without complete solution of the electromagnetic radiation field, the derivation of the absolute optical-power emission and of the angular-radiation pattern requires a detailed solution for the electromagnetic fields in the presence of the electron beam, as was done in Ref. 14. The translation symmetry in the y direction, which allowed us to define the radiation modes with a single wave number k_y, also permits separation into two different modes: the E polarization, for which $\mathcal{E}_y \neq 0, \mathcal{H}_y = 0$, and the M polarization, for which $\mathcal{E}_y = 0, \mathcal{H}_y \neq 0$. All the field components of the E polarization can be presented in terms of $\mathcal{E}_{yn}$:

$$\begin{aligned} \mathcal{E}_{yn} &\equiv \phi_n(k_y, \omega), \\ \mathcal{E}_{xn} &= -\frac{k_y k_{xn}}{k^2 - k_y{}^2}\phi_n, \\ \mathcal{E}_{zn} &= -\frac{k_y k_{zn}}{k^2 - k_y{}^2}\phi_n, \\ \mathcal{H}_{xn} &= -\sqrt{\frac{\epsilon_0}{\mu_0}}\frac{kk_{zn}}{k^2 - k_y{}^2}\phi_n, \\ \mathcal{H}_{yn} &= 0, \\ \mathcal{H}_{zn} &= \sqrt{\frac{\epsilon_0}{\mu_0}}\frac{kk_{xn}}{k^2 - k_y{}^2}\phi_n. \end{aligned} \tag{7}$$

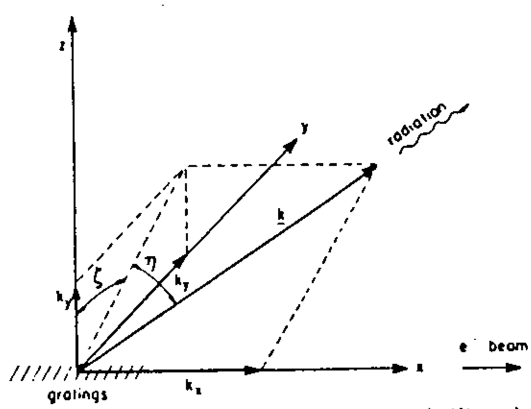

Fig. 2. Definition of the latitude (η) and azimuth (ζ) angles of a Smith–Purcell diffraction order.

All the field components of the M polarization may be presented in terms of $\mathcal{H}_{yn}$:

$$\mathcal{H}_{yn} \equiv \psi_n(k_y, \omega),$$

$$\mathcal{H}_{xn} = -\frac{k_y k_{xn}}{k^2 - k_y^2}\psi_n,$$

$$\mathcal{H}_{zn} = -\frac{k_y k_{zn}}{k^2 - k_y^2}\psi_n,$$

$$\mathcal{E}_{xn} = \sqrt{\frac{\mu_0}{\epsilon_0}}\frac{k k_{zn}}{k^2 - k_y^2}\psi_n,$$

$$\mathcal{E}_{yn} = 0,$$

$$\mathcal{E}_{zn} = -\sqrt{\frac{\mu_0}{\epsilon_0}}\frac{k k_{xn}}{k^2 - k_y^2}\psi_n. \tag{8}$$

The Poynting-vector power density of the n-order *radiating* space harmonic propagates in the direction of the $\mathbf{k}_n$ propagation vector and is given by

$$\tfrac{1}{2}\mathcal{E}_n \times \mathcal{H}_n^* = \tfrac{1}{2}(k^2 - k_y^2)^{-1}\omega\,(\epsilon_0\phi_n\phi_n^* + \mu_0\psi_n\psi_n^*)\mathbf{k}_n. \tag{9}$$

The energy that is lost by a single electron by radiation when traversing one period length D is found to be the sum of the z components of the Poynting-vector powers [Eq. (9)] of all radiating space harmonics integrated over all ω and k_z and multiplied by D:

$$W = \frac{e^2}{D\epsilon_0}\sum_{\substack{\text{radiating}\\ \text{waves } n}}\int_{-\pi/2}^{\pi/2}\int^{\pi/2}\frac{\cos^2\eta\cos^2\zeta}{[(1/\beta) - \sin\eta]^3}|R_n(\zeta,\eta)|^2 \times \exp\left[-\frac{z_0 - z_{\max}}{h_{\text{int},n}(\zeta,\eta)}\right]\cos\eta\, d\eta d\zeta, \tag{10}$$

where

$$h_{\text{int},n} \equiv \frac{D(\beta^{-1} - \sin\eta)}{4\pi n[\beta^{-2} - 1 + \cos^2\eta\sin^2\zeta]^{1/2}} = \frac{\lambda_n}{4\pi[\beta^{-2} - 1 + \cos^2\eta\sin^2\zeta]^{1/2}}. \tag{11}$$

The parameter $|R_n(\zeta,\eta)|^2$ can be calculated from ϕ_n, ψ_n after these functions are computed from the equations that result by matching boundary conditions at the beam position $z = z_0$ and at the grating surface. Assuming an ideal-conductor sinusoidal grating, Van den Berg numerically computed the parameter $R_{-1}(\zeta,\eta)$ and illustrated it for various values of $\beta \equiv v_0/c$ and of h/D.[14]

The parameter $h_{\text{int}}(\zeta,\eta)$ is the effective interaction range. Only electrons that pass within the interaction range above the grating $z_0 - z_{\max} < h_{\text{int}}(\zeta,\eta)$ contribute effectively to the n-order Smith–Purcell radiation in the (ζ,η) direction. For a nonrelativistic or a moderately relativistic electron beam, h_{int} is a fraction of a wavelength. Thus, at the optical wavelength, only a small portion of the electron-beam current is effective in the interaction, and the radiation is weak.

The integrand of Eq. (10) is the radiative energy emitted in direction (η,ζ) per period length D per solid angle. Assuming that the electron beam fills the region above $z = z_{\max}$ up to a height well above $z_{\max} + h_{\text{int}}$ with uniform current density J_0, the power emitted by the total beam at direction (η,ζ) per unit solid angle is obtained by multiplying this integrand by the electrons' flux density J_0/e, the electron-beam width b, and the number of periods in the gratings L/D and then by integrating over z from $z_{\max}$ to infinity:

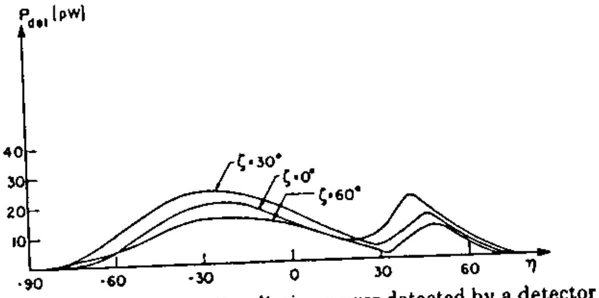

Fig. 3. The Smith–Purcell radiation power detected by a detector as a function of η for various azimuth angles ζ as calculated from Van den Berg's graphs for grating and beam parameters corresponding to the experiment.

$$I_n(\zeta,\eta) = \frac{eJ_0bL}{4\pi\epsilon_0 Dn} \times \frac{\cos^2\eta\cos^2\zeta}{(\beta^{-1} - \sin\eta)^2(\beta^{-2} - 1 + \cos^2\eta\sin^2\zeta)^{1/2}} \times |R_n(\zeta,\eta)|^2. \tag{12}$$

Figure 3 illustrates the theoretical angular power distribution $P_{\text{det}}(\zeta,\eta) = I_n(\zeta,\eta)\Omega_{\text{det}}$ that is expected to be collected by a detector placed at angle (ζ,η) according to Van den Berg's theory and to the assumed parameters of our experiment. The radiation factor $|R_{-1}(\zeta,\eta)|^2$ was calculated for the experimental parameters by interpolation of the parameter values given by Van den Berg. The assumed experimental parameters of Fig. 3 are $h/D = 1/3$, $E = 100$ keV ($\beta = 0.55$), the solid angle intercepted by the detector $\Omega_{\text{det}} = 0.005$ sr, $J_0 = 0.8$ mA/cm^2, beam width $b = 0.2$ mm, $1/d = 3600$ lines/mm, $n = -1$, and $L = 2.5$ cm.

Although Fig. 3 is based on a crude interpolation, we believe that it reflects the gross features and the approximate quantitative values of the radiation pattern as predicted by Van den Berg's theory. The minimum of the curves around $\eta = 30°$ corresponds well to the Doppler-shifted (realistic-transformation) node of a purely transversely oscillating moving dipole: $\eta_{\min} = \arcsin(\beta_0) = 32°$. The curves also feature a maximum for the radiation pattern as a function of ζ that occurs for each latitude angle η at a different azimuthal angle ζ, $0° < \zeta < 90°$.

SALISBURY'S MODEL

An alternative physical mechanism was suggested by Salisbury to explain Smith–Purcell radiation.[12] According to Salisbury's model, the electrons hit the grating at a small angle and are reflected at the top of the grating rulings, producing thin, parallel sheet beamlets with a period along the x axis that is equal to the grating's period (see Fig. 4). According to Salisbury's model, the periodic space-charge field of these sheet beamlets operates as a wiggler on the incoming electrons

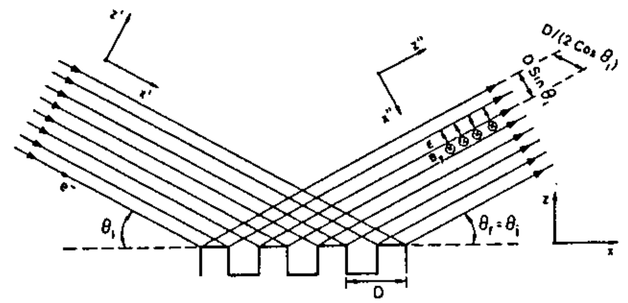

Fig. 4. Configuration of Salisbury's radiation mechanism.

in the beam. Although this possible mechanism should be weak (because the space-charge field of the beam is expected to be small), it has the favorable feature that the interaction length limitation [Eq. (11)] is eliminated, and the entire cross section of the beam is capable of participating in the interaction. Salisbury's model has not yet been confirmed or discarded by an independent study to our knowledge. As we show here by careful computation of the effect predicted by Salisbury's model, this model is inappropriate for explaining the radiation power levels measured in our experiment and probably in other similar experiments.

The current density and the space-charge density modulation of the sheet-current beamlets are taken to be $J_0 \cos[2x''/(D \sin \theta_i)]$ and $(J_0/v_0) \cos[2\pi x''/(D \sin \theta_i)]$, respectively, where x'' is a coordinate perpendicular to the current sheets (see Fig. 4). The space-charge field in the direction of the incoming electron beam and in the perpendicular direction and the magnetic field are integrated directly from Maxwell equations:

$$E_{x'} = \frac{1}{2\pi} \sqrt{\frac{\mu_0}{\epsilon_0}} \frac{J_0}{\beta_0} D \sin(\theta_i) \sin(2\theta_i) \sin\left(\frac{4\pi \cos \theta_i}{D} x'\right), \tag{13}$$

$$E_{z'} = \frac{1}{2\pi} \sqrt{\frac{\mu_0}{\epsilon_0}} \frac{J_0}{\beta_0} D \sin(\theta_i) \cos(2\theta_i) \sin\left(\frac{4\pi \cos \theta_i}{D} x'\right), \tag{14}$$

$$B_{y'} = \frac{1}{2\pi c} \sqrt{\frac{\mu_0}{\epsilon_0}} J_0 D \sin(\theta_i) \sin\left(\frac{4\pi \cos \theta_i}{D} x'\right). \tag{15}$$

In the limit of grazing incidence ($\theta_i \ll \pi$), in which most Smith–Purcell experiments are conducted, the period of the wiggling forces that are experienced by the electrons is $D/2$. Consequently, it turns out that the radiation orders (which result from the periodic wiggler synchrotron radiation generated by the periodic forces) will coincide with only the even orders of the Smith–Purcell radiation given by Eq. (1). Thus radiation of the first order is not explained by this mechanism.

When $\theta_i \ll \pi$, the longitudinal electric-yield modulation E_x diminishes relative to the transverse field E_z. Furthermore, for relativistic beams, the transverse Lorentz force ev_0B_y, which was ignored by Salisbury altogether, is comparable with the transverse electric force eE_z (reduced by a factor β^2). They both go to zero in proportion to θ_i where $\theta_i \ll \pi$.

The spontaneous-emission theory of magnetic bremsstrahlung (synchrotron radiation) FEL's[17] can be adopted straighforwardly to describe the spontaneous emission resulting from the transverse wiggling force $e(E_x, +v_0B_y)$. In terms of the angle coordinates (ζ, η), the radiation pattern is given by

$$I(\zeta, \eta) = \frac{eI_0 a_w^2 k_w^2 L}{32\pi^2 \epsilon_0 \gamma^2 \beta^2} \times \frac{\cos^2 \zeta(\beta^{-1} - \sin \eta)^2 + \sin^2 \zeta(\beta^{-1} \sin \eta - 1)^2}{(\beta^{-1} - \sin \eta)^5}, \tag{16}$$

where

$$\gamma \equiv (1 - \beta^2)^{-1/2},$$

$$a_w \equiv \frac{e}{k_w mc}\left(B_w + \frac{1}{v_0} E_w\right), = \frac{eDJ_0\sqrt{\mu_0/\epsilon_0} \sin \theta_i}{2\pi k_w mc^2} (1 + 1/\beta_0^2) \tag{17}$$

and $k_w = 4\pi/D$.

We calculated the power distribution $P_{\rm det}(\zeta, \eta) = I(\zeta, \eta)\Omega_{\rm det}$ that would be predicted by Eq. (16) by using the same experimental parameters as above. The radiation pattern exhibits behavior similar to that predicted by Van den Berg's model, including the dip at angle $\eta = \arcsin \beta = 32°$; however, the absolute power emission is significantly smaller. Even for large incidence angle $\theta_i = 1°$, the power collected by the detector should be 5×10^{-41} W multiplied by the angular-dependence factor of Eq. (16). This is much smaller than the power predicted in Fig. 3. It is also significantly smaller than the minimum power that can be detected by our detector.

EXPERIMENTAL PROCEDURE AND RESULTS

We used a Philips EM300 electron microscope to produce a 0.25-μA, 200-μm-diameter circular electron beam. The divergence of the beam was less than 1 mrad, and the beam voltage was 60, 80, or 100 keV (β = 0.443, 0.503 and 0.550, respectively). The grating that we used was a 2.5-cm × 2.5-cm (1-in. × 1-in.) aluminum-coated replica grating with 1800 ruling lines/mm. The radiation was detected by using a sensitive Hamamtsu R 936 photomultiplier.

The power that was detected was calibrated by using photomultiplier response curves and by taking into consideration the window absorption.

The measured Smith–Purcell power in the −2 diffraction order is drawn in Fig. 5 versus angle ζ at 100 keV for $\eta = 0°$,

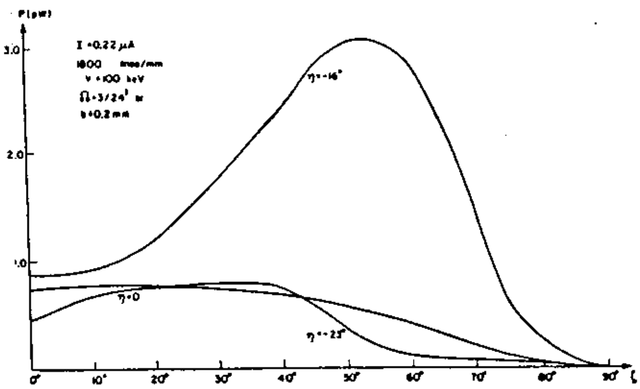

Fig. 5. Measured −2-order Smith–Purcell radiation power as a function of the azimuth angle ζ.

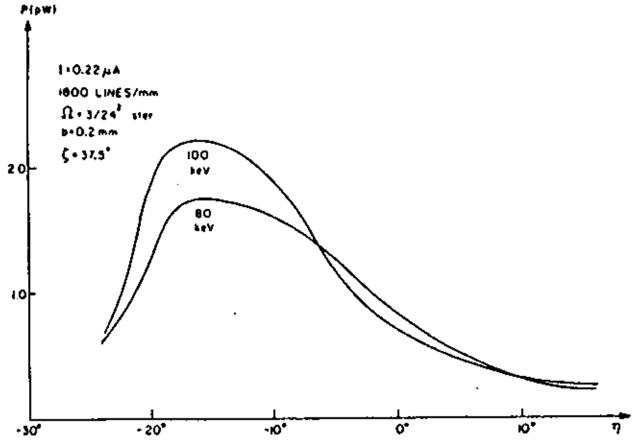

Fig. 6. Measured −2-order Smith–Purcell radiation power as a function of the latitude angle η.

−16°, and −23°. The variation of the measured power versus the angle η at a fixed $\zeta = 37.5$ is presented in Fig. 6. We also measured Smith–Purcell power versus electron energy β (for 60, 80 and 100 keV), and we found, in accordance with most existing theories for the Smith–Purcell effect, that the power increased rapidly with increasing β. When β went from 0.443 to 0.550, the power was tripled.

DISCUSSION

The main features of the radiation distribution, which was measured as a function of (ζ, η) (Figs. 5 and 6), agree quite well with Van den Berg's theoretical model for Smith–Purcell radiation (Fig. 3). The measured absolute power levels are about an order of magnitude lower than the theoretical prediction. Since Van den Berg's analysis was made for −1-order diffraction from an ideal-conductor sinusoidal grating, its application to our experiment for a blazed grating and for −2-order diffraction should not give more than the main features of the radiation pattern and the order of magnitude or the upper limit values for the radiation power.

The experimental confirmation of the dispersion relation [Eq. (1)] was evident. We also verified that the radiation wavelength did not change as a function of ζ and was dependent only on η. Nevertheless, this by itself is not a check for the validity of the theoretical model or even of the physical mechanism. Toraldo di Francia's model[13] would predict exactly the same dispersion relation, but his prediction for the angular power distribution and the power levels deviates substantially from the measured parameters. As we mentioned above, confirmation of the dispersion relation [Eq. (1)] in the second order is also consistent with Salisbury's model, and so is the radiation pattern measured. However, the absolute value of the radiation power predicted by Salisbury's model is so much smaller than the measured power that it must be rejected as a possible explanation for our experiment or for similar ones.

An important feature of the computed and the measured radiation distribution curves is the fact that the radiated power peaks at azimuthal angles $\zeta \neq 0$. This has substantial relevance to the design of Smith–Purcell FELS's, since we suspect that the stimulated emission also increases in the radiation directions in which the spontaneous Smith–Purcell radiation is high.[1,2] Thus, in an open resonator Smith–Purcell FEL, it may be advantageous to build the resonator from three or five mirrors. One mirror is the grating itself, and the others are placed at directions $(\pm\zeta_m, \pm\eta_m)$, where ζ_m is the angle of maximum emission [see Fig. 7(a)]. In millimeter-wavelength orotron devices,[6–9] the resonator is made out of a grating and a convex mirror right above it ($\zeta = 0, \eta = 0$). We suggest that in this device it may also be preferable to replace the convex mirror by two mirrors at angles ($\zeta = \pm\zeta_m, \eta = 0$).

In a Smith–Purcell FEL based on a rectangular waveguide, it may be preferable to choose waveguide modes that have zigzag bouncing angles close to ζ_m [see Fig. 7(b)]. In the infrared regimes, the waveguide modes are leaky modes whose losses are strongly dependent on the mode zigzag angles. If the waveguide is largely overmoded, the mode losses may be small enough to be used in a laser oscillator or in an amplifier configuration.

Rectangular waveguides seem to be most appropriate for Smith–Purcell FEL's since they incorporate the gratings as one of the waveguide walls. The leaky modes of a rectangular metal-dielectric waveguide (longitudinal section magnetic and longitudinal section electric) are identical with the E-type and the H-type modes given in Eqs. (7) and (8), except that the transverse wave numbers k_x and k_y are quantized by the finite dimensions of the guide cross section $k_y = p\pi/w_y$, $k_z = q\pi/w_z$. In a hollow rectangular waveguide, the high-order leaky eigenmodes are hybrid modes EH_{qp}.[18] The field attenuation constant of such modes is given by

$$\alpha_{pq} = \frac{2\pi^2}{k^2}\left[\frac{p^2}{w_y{}^3}\mathrm{Re}\left(\frac{1}{\sqrt{\nu^2-1}}\right) + \frac{q^2}{w_z{}^3}\mathrm{Re}\left(\frac{\nu^2}{\sqrt{\nu^2-1}}\right)\right], \quad (18)$$

where ν is the complex index of refraction of the waveguide walls.

For a high-order mode in an overmoded waveguide, we may substitute $p = k_y w_y/\pi$ and $q = k_z w_z/\pi$ and use Eq. (6).

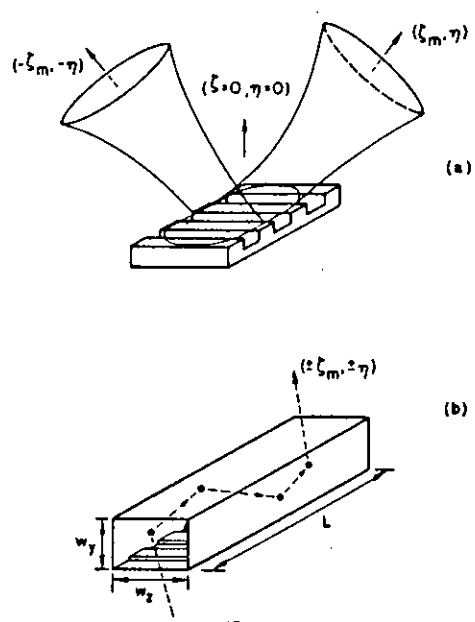

Fig. 7. Proposed optimal resonator configurations for Smith–Purcell FEL's. (a) Three-mirror open-cavity resonator. (b) Rectangular waveguide or closed-cavity resonator.

Hence

$$\alpha_{pq} = 2\cos^2\eta\left[\frac{\sin^2\zeta}{w_y}\mathrm{Re}\left(\frac{1}{\sqrt{\nu^2-1}}\right)+\frac{\cos^2\zeta}{w_z}\mathrm{Re}\left(\frac{\nu^2}{\sqrt{\nu^2-1}}\right)\right]. \tag{19}$$

For a given operating wavelength λ, a diffraction order n, and a beam velocity v_0, η is determined uniquely by the dispersion relation [Eq. (1)]. The freedom to choose ζ, w_y, and w_z allows for the designing of a FEL cavity with low mode attenuation. Generally, $\mathrm{Re}(\nu^2/\sqrt{\nu^2-1}) > \mathrm{Re}(1/\sqrt{\nu^2-1})$. For this reason it is preferable to choose a large ζ in order to keep the second term in Eq. (19) small. This is favorably consistent with the fact that stronger emission is also expected at a higher value of ζ. In a Smith–Purcell FEL design it is expected that the zigzag angle will be chosen near the maximum emission angle $\zeta \simeq \zeta_m$. The choice of waveguide cross-section dimensions then gives a degree of freedom for minimizing waveguide attenuation of the preferable mode.

ACKNOWLEDGMENTS

We acknowledge the valuable technical assistance of T. van der Hagen and H. Kleinman. E. Grunbaum and Y. Larea kindly made the electron microscope available to us and helped to operate it. We also had useful communications with G. Hughes of Auburn University, Auburn, Alabama, and J. P. Bachheimer of Laboratoire de Spectrometrie Physique, Grenoble, France. We also thank R. Erdmann of P.T.R. Corporation for special consideration in supplying gratings for the experiment.

This research was supported by the U. S. Air Force Office of Scientific Research under grant 82-239.

REFERENCES

1. J. M. J. Madey, Nuovo Cimento B 50, 64 (1979).
2. A. Gover, A. Friedman, S. Ruschin, G. Kuritzki, and A. Yariv. Faculty of Engineering, Quantum Electronics Laboratory Rep. 84/2 (Tel Aviv University, Tel Aviv, Israel, to be published). This paper derives the general relation between the spontaneous emission radiant intensity and the stimulated emission gain of any quasi-free-electron radiation scheme. The report is available on request.
3. A. Gover and A. Yariv, *Physics of Quantum Electronics*, S. Jacobs, M. Sargent III, and M. Scully, eds. (Addison-Wesley, Reading, Mass., 1977), Vol. 5, p. 197.
4. A. Gover and Z. Livni, Opt. Commun. 26, 375 (1978).
5. J. Wachtel, J. Appl. Phys. 50, 49 (1979).
6. F. S. Rusin and G. D. Bogomolov, Proc. IEEE 57, 720 (1969).
7. V. K. Korneyekov and V. P. Shestopolov, Sov. Radio Eng. Elect. Phys. 22, 148 (1977).
8. K. Mizuno, S. Ono, and Y. Shibata, IEEE Trans. Electron Devices ED-20, 749 (1973).
9. R. P. Levitt, D. E. Wortman, and H. Dropkin, IEEE J. Quantum Electron. QE-17, 1333, 1341 (1981).
10. S. J. Smith and E. M. Purcell, Phys. Rev. 92, 1069 (1953).
11. K. Ishiguro and T. Tako, Opt. Acta 8, 25 (1961).
12. W. W. Salisbury, J. Opt. Soc. Am. 60, 1279 (1970).
13. G. Toraldo di Francia, Nuovo Cimento 16, 61 (1960).
14. P. M. van den Berg, J. Opt. Soc. Am. 63, 1588 (1973).
15. J. P. Bachheimer, Phys. Rev. B 6, 2985 (1972).
16. E. L. Burdette and G. Hughes, Phys. Rev. A 14, 1766 (1976).
17. A. Gover, H. Freund, V. L. Granatstein, J. H. McAdoo, and C. M. Tang, *Millimeter Components and Techniques*, Part III of *Infrared and Millimeter Waves*, Vol. 12, K. J. Button, ed. (Academic, New York, to be published). Equation (16) can also be derived by integration over frequencies of the spectral radiant intensity of undulator radiation [e.g., see B. M. Kincaid, J. Appl. Phys. 48, 2684 (1977)].
18. B. Adam and F. Kneubuhl, Appl. Phys. 8, 281 (1975).